Potentiostatic formation of porous silicon in dilute HF: Evidence that nanocrystal size is not restricted by quantum confinement

T.L. Sudesh L. Wijesinghe [a,1], E.J. Teo [b], D.J. Blackwood [a,*,1]

[a] *Department of Materials Science and Engineering, National University of Singapore, Block E3A, 7 Engineering Drive 1, Singapore 117574, Singapore*
[b] *Department of Physics, 2 Science Drive 3, National University of Singapore, Singapore 117542, Singapore*

Abstract

The role that applied potential has in controlling the properties of porous silicon formed on highly conductive p-type silicon in diluted HF has been investigated by studying the photoluminescence characteristics along the current–voltage curve and using high resolution transmission electron microscopy (HRTEM) evidence to support the conclusions drawn. A dramatic decrease in the average nanocrystal size was found to take place after the etching current density switched from an exponential dependence on the applied potential to a linear relationship. Importantly this event occurred prior to reaching the U_{ps} potential (usually consider the onset of electropolishing). This rapid decrease in particle sizes has been explained in terms of the partial formation of an oxide film. The presence of oxygen terminated porous silicon allows a trapped exciton states model to be invoked, which removes the quantum confinement restrictions on the minimum particle size. Support for the presence of a partial oxide prior to U_{ps} comes from both FTIR measurements and previous literature related to the location of the flat-band potential.
© 2008 Elsevier Ltd. All rights reserved.

Keywords: Porous silicon; Current–voltage curve; Photoluminescence; HRTEM; Quantum confinement

1. Introduction

Porous silicon (PSi) formation and its controlling electrochemistry have been intensely studied over the last 15 years. Throughout this time the validity of the quantum confinement effect to explain correlations between photoluminescence (PL) energy and the size of the PSi nanocrystal has been debated at length [1–8]. However, there are still some disagreements, particularly with regards to the blue-shift observed at high current densities [9–15]. Adachi and Oi have recently argued that the quantum confinement makes possible quasidirect transitions at and above the indirect absorption edge. Many electronic states would be available to participate in these quasidirect transitions, arising from enhanced momentum fluctuations Δk due to the uncertainty principles in nanocrystallites, which accounts for the broad PL emission observed [16].

PSi is usually obtained by electrochemical etching of silicon wafers in HF solution, a process that has been broadly explained in several previous works [2–4]. The basic characteristics of the current–voltage (*I–V*) curve are that initially the current rises exponentially with the applied potential, the region in which the PSi is formed, which leads into a linear region and at some critical potential, U_{ps}, the current density moves through a peak, J_{ps}, which in most of the literatures is assigned to the onset of oxide formation. Next, possibly after a small plateau region, the current density again rises sharply, marking the onset of electropolishing, which is controlled by the chemical dissolution of the oxide in the fluoride solution [5]. The rate limiting steps for PSi formation and the electropolishing are thought to be electrochemical charge transfer at the Si/electrolyte interface and dissolution of silicon oxide, respectively [6].

Although potential is undoubtedly an important parameter in controlling the properties of PSi, most previous investigations have been carried out galvanostatically, as opposed to potentiostatically, due to the difficulty of working with reference electrodes in HF solutions. A general trend of increasing porosity with increasing anodising current density for p-type Si has been widely reported and correlated to the quantum con-

* Corresponding author. Tel.: +65 65166289; fax: +65 67763604.
 E-mail address: msedjb@nus.edu.sg (D.J. Blackwood).
[1] ISE member.

finement hypothesis [7,8,17]. Ohmukai and Tsutsumi observed a strong dependence of PL intensity on the current density even for a constant total charge, i.e. the same number of Si atoms was removed from each sample [9]. Koyama reported that in extremely dilute HF the PL intensity is determined by the ratio of the etching current density to that of the J_{ps} peak, leading him to suggest that the presence of silicon oxides plays an important role in the formation of luminescent Si nanostructures in PSi layers [7]. The aim of this paper is to investigate the role that the applied potential has in controlling the properties of PSi formed on highly conductive p-type Si in diluted HF by studying the PL characteristics along the *I–V* curve and using HRTEM evidence and FTIR spectra to support the conclusions drawn.

2. Experimental

PSi was formed on p-type, 0.015 Ω cm resistivity (Virginia Semiconductors), (1 0 0) oriented wafers by etching in a solution of 2.7 wt% HF dissolved in a 1:2 mixture of H_2O and ethanol. A standard three-electrode system was used with a Si working electrode, a platinum mesh counter electrode and a saturated calomel reference electrode. The reference electrode was furnished with a polyethylene luggin capillary with the tip positioned at around 5 mm distance from the working electrode. All potentials quoted in this paper are versus saturated calomel electrode (SCE) and have been corrected for the uncompensated solution resistance (IR drop). The silicon wafers were potentiodynamically polarised from −1000 mV at a sweep rate of 5 mV/s, using the potentiostat and sweep generator components of an ACM Instruments field machine. The samples for PL measurements and transmission electron microscopy (TEM) investigations were swept to holding potentials within either the PSi or electropolishing regions and held for a period of 10 min; during this holding period the current density fell by less than 2%. After etching in the HF solution the samples were rinsed in ethanol and blown dry by N_2 gas and then immediately transferred to a portable vacuum chamber to be transported to the PL or Fourier transform infrared (FTIR) spectrometers.

For PL the samples were removed from the vacuum portable chamber and immediately placed under the microscope. It took approximately 30 s to record the first spectra, but as several different points on a single specimen's surface were probed the samples were exposed to air for several minutes before the last spectrum was recorded; note that there was no obvious trend in either the PL intensity or the peak wavelength with the time exposed to the atmosphere.

For the FTIR, after removal from the portable vacuum chamber the samples were placed into a nitrogen purged sample chamber and spectra collected immediately; there being approximately 45 s elapsing from the time the samples were removed from the vacuum chamber and the spectra collected.

However, because there have been reports that the oxidation of PSi can occur within seconds to a minute of exposure to atmospheric conditions, a few samples were prepared under even more stringent conditions [14]. These involved performing the etching and rinsing (now using N_2 purged ethanol) of the silicon and its subsequent transfer to the portable vacuum cham-

ber under a nitrogen blanket, i.e. a constant stream of nitrogen blown down, through a funnel, over the working area (about 30 cm × 30 cm). Furthermore, a nitrogen blanket was applied continuously during the collection of the PL spectra. However, no additional changes were made to the FTIR arrangement as this was already conducted in a N_2 atmosphere.

PL spectrometer consisted of a coherent 405 nm blue diode laser with 50 mW power was focused onto the samples through a Nikon Eclipse LV150 microscope with a 50× objective. The PL was detected using a charge coupled device (CCD) Ocean Optics spectrometer via an optical fibre. The laser light was cut-off from the PL signal using a 470-nm long pass filter (Nikon BV-2A). Typically PL spectra were collected from five different locations on a sample's surface. FTIR spectra were collected in reflectance mode on a Varian 3100 spectrometer at a resolution 8 cm^{-1} with background spectra being collected from the back side (unpolished) of a silicon wafer.

The TEM samples were prepared in a similar manner to that reported by Cullis and Canham [18] except the PSi was not allowed to fall directly onto the copper grids. Instead these grids were dipped into ethanol and then touched gently onto the removed PSi, thereby picking it up. The HRTEM used was a JEOL JEM 3010 HRTEM operated at 300 kV. PSi film thicknesses were estimated from X-sections analysed in a Philips XL 30 field emission gun scanning electron microscope (SEM) operated at 30 kV.

3. Results

An *I–V* curve for 0.015 Ω cm, p-type anodised in 2.7% HF is shown in Fig. 1, line (a). Initially the *I–V* curve follows the expected trend, with the current density increasing exponentially with potential from around −50 mV, as the PSi starts to form, and then switching to an almost linear relationship at about 35–40 mV. However, at approximately 90 mV, with the current density at 10.4 mA/cm^2, a significant decrease in *I–V* slope is observed, but no obvious J_{ps} peak. Conversely, such a peak can be obtained by the addition of 0.5 M NH_4Cl to the solution (Fig. 1, line (b)) and occurs at the same potential as the decrease in slope is observed in the *I–V* curve without NH_4Cl (Fig. 1, line (a)), suggesting that the two features have the same original, i.e. J_{ps} in the absence of NH_4Cl is only 10.4 mA/cm^2. It is not known why the presence of NH_4Cl is required to obtain a full J_{ps} peak, presumably it influences the solubility of the oxide film; the NH_4Cl did reduce the uncompensated resistance from approximately 50 Ω to about 10 Ω. The J_{ps} current density recorded with 0.5 M NH_4Cl at 16.7 mA/cm^2 is in excellent agreement with the predicted value for 2.7 wt% HF [2]. Note that the authors do not know if the J_{ps} values quoted in Ref. [2] for low HF concentrations were collected in the presence or absence of NH_4Cl.

Fig. 2 shows representative PL spectra collected at different potential limits (without NH_4Cl), with the relevant current densities and PL peak wavelengths being tabulated in Table 1; there was some variation in the PL wavelength maximum with location of the laser illumination on the PSi surface, thus ranges are shown in the table. Broad and almost identical PL spectra
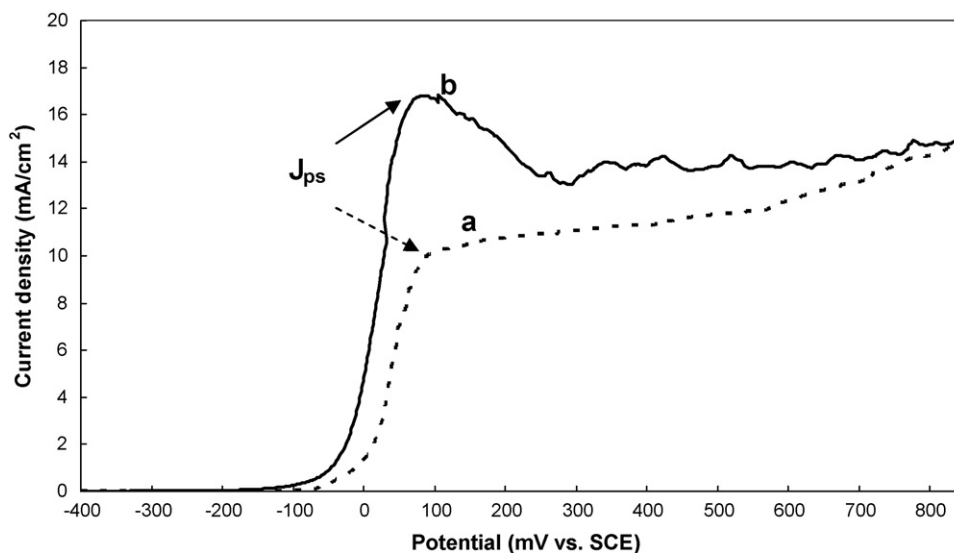
Fig. 1. Potentiodynamic polarisation curves for 0.015 Ω cm p-type etched in (a) 2.7% HF (dashed line) and (b) 2.7% HF + 0.5 M NH4Cl (solid line). Both plots are corrected for IR drop.
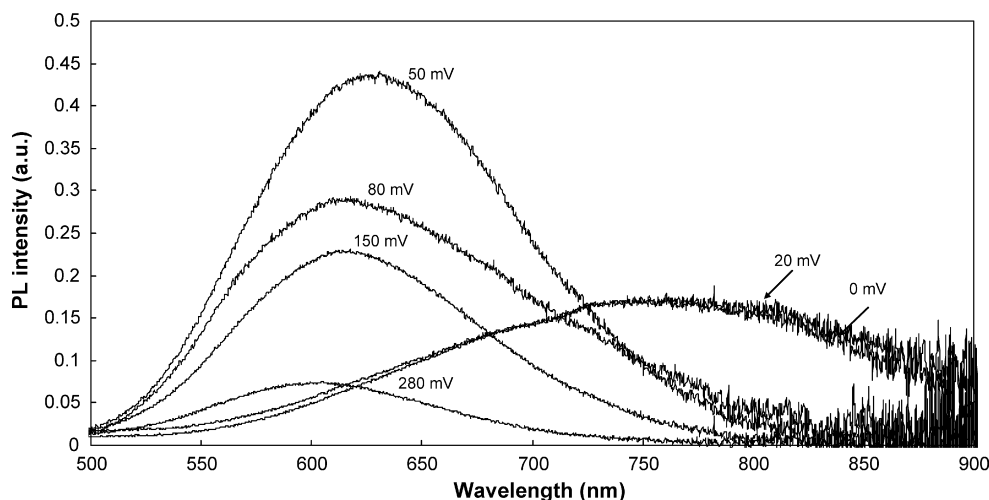

Fig. 2. PL spectra for 0.015 Ω cm p-type etched in 2.7% HF at different potentials.

were recorded for 0 mV and 20 mV. On reaching a potential of 50 mV the PL intensity increased sharply (by more than a factor of 2) and its wavelength maximum blue shifted (from ∼760 nm to ∼620 nm); note that this jump in the PL spectra

Table 1
The current density and PL peak wavelength for each sample etched at particular potential in 2.7% HF

Applied potential (mV vs. SCE)	Current density (mA/cm^2) ±0.10	PL peak wavelengths (nm)
0	1.4	755–760
20	2.6	755–760
50	7.0	615–630
65	8.6	610–620
80	9.6	605–615
150	10.5	600–610
280	11.0	590–600
400	11.5	No PL

For each sample around 6 spots were tested for PL.

occurs just after the I–V curve changes from exponential to linear behaviour. Further increasing the potential beyond 50 mV caused the PL intensity to decrease, but the blue-shifting continued up to 280 mV. No PL was observed at potentials equal to or above 400 mV. Applying the additional precautions to prevent atmospheric oxidation, i.e. the N_2 blanket described in Section 2, had no significant influence on the recorded PL spectra.

Interestingly, the complete loss of PL appears to coincide with the end of the J_{ps} peak seen in the presence of NH_4Cl (Fig. 1, line (b)) that may mark the formation of a complete oxide layer. The potential dependence of the PL intensity, which can be observed from Fig. 2, correlates well with the film thicknesses determined by SEM X-sections given in Table 2, which is in agreement with previous publications [19,20].

Fig. 3(a) and (b) shows representation HRTEM images of PSi samples collected at different potential limits along the I–V curve. At all potentials a large size range, from 1.5 nm to 25 nm, of nanocrystals was seen. The larger nanocrystals are of irregu-

Table 2
Thicknesses[a] of the PSi layers and size distribution of nanocrystals as a percentage out of total nanocrystallites present in each sample

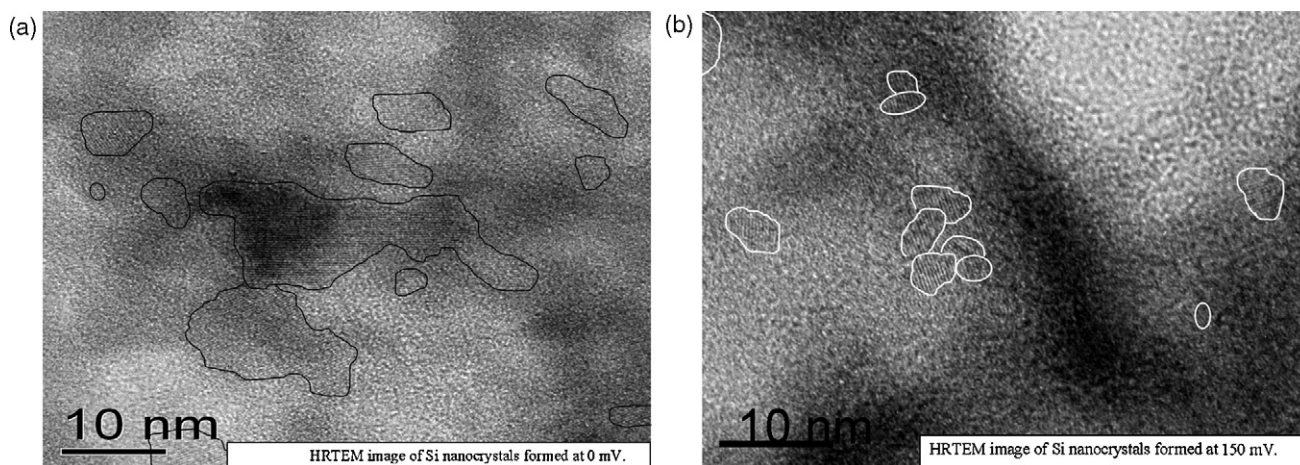| Potential (mV vs. SCE)	Thickness (nm)	Size range of nanocrystallites (l = longest length) (nm)			
		$l < 3$	$3 < l < 5$	$5 < l < 10$	$l > 10$
0	210	6%	35.8%	34.4%	23.8%
20	258	6.3%	35.7%	34.3%	23.7%
80	430	29.5%	42.8%	23.9%	3.8%
150	130	45.9%	33.7%	19.4%	1.0%

[a] Thickness was calculated using SEM cross-sectional images.

Fig. 3. (a) HRTEM image of Si nanocrystals formed at 0 mV and (b) HRTEM image of Si nanocrystals formed at 150 mV.

lar shape, but become more ellipsoidal with decreasing size. The wide nanocrystal size distribution is consistent with the broad PL spectra recorded (Fig. 2) [2,3]. By measuring along the long axis of the nanocrystals, these were classified into four size distributions: (a) larger than 10 nm, (b) 5–10 nm, (c) 3–5 nm and (d) less than 3 nm. Note that the smallest ellipsoidal nanoparticles observable under the HRTEM had elongated axes of ~1.5 nm. Table 2 shows the size distribution of nanocrystals as a percentage of total nanocrystals observed under the HRTEM from samples formed at four different potential limits with the same data being presented graphically in Fig. 4. At least 20 HRTEM images were recorded and analysed at each potential limit. It is

clear from the data in Table 2 and Fig. 4 that the fraction of the PSi particles within the two smallest size ranges increases dramatically as the potential increases from 20 mV to 80 mV. According to the quantum confinement model a decrease in nanocrystallite size should cause a blue-shift in the PL, as such the TEM data are in good agreement with the recorded PL spectra.

Fig. 5a shows FTIR reflectance spectra collected from PSi samples formed at 0 mV and 80 mV. At the lower potential the Si–H stretching bands at ~2100 cm^{-1} can be seen, whilst at 80 mV the appearance of a Si–O stretching band near 1170 cm^{-1} is evidence for partial oxidation, despite being negative of the U_{ps} potential (90 mV). However, the Si–H stretching bands
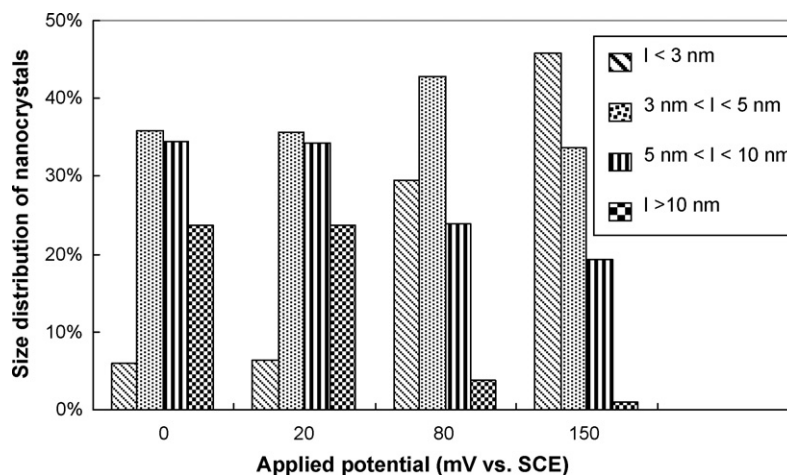

Fig. 4. Size distribution of nanocrystals as a percentage of total nanocrystals observed under the HRTEM from samples formed at four different potential limits.
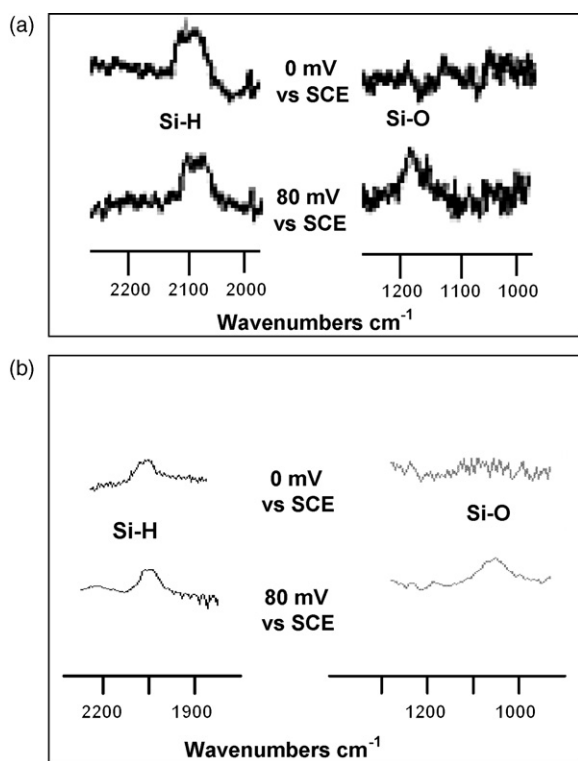
Fig. 5. (a) FTIR reflectance spectra collected from PSi samples formed at 0 mV and 80 mV and (b) FTIR reflectance spectra collected from PSi samples formed at 0 mV and 80 mV under a N_2 blanket.

remain visible in the 80 mV spectrum indicating that oxidation is not complete. Applying the additional precaution to prevent atmospheric oxidation of etching under a N_2 blanket had no significant influence on FTIR spectra recorded at 0 mV (this was expected as no oxide had been observed at this potential). At 80 mV evidence for an oxide film was still seen, however, the Si–O stretch was shifted from 1170 cm^{-1} to 1050 cm^{-1}, but without any significant change in intensity (Fig. 5b). The explanation for this shift is that there are two modes for the Si–O stretch; a perpendicular mode that increases in frequency from ~1170 cm^{-1} to ~1230 cm^{-1} as the oxide thickens and a parallel mode at about 1050 cm^{-1} which is usually dominant and independent of thickness.

4. Discussion

The most striking observation evident from both the PL spectra and the HRTEM analysis is that the average size of the PSi nanocrystals does not decrease gradually with increasing applied current density/voltage rather it undergoes a dramatic decrease prior to reaching the U_{ps} potential, with an obvious proliferation in the number of sub 3 nm diameter nanocrystals being observed. Outside of this critical potential range the average size of the PSi nanocrystals decreased slowly and gradually with increasing potential.

Allongue et al. [21] proposed that in the anodization of silicon in hydrofluoric acid two holes are first required to convert a Si–H bond to a Si–OH bond and then either this is chemically replaced by a Si–F bond, yielding PSi, or further holes reach the

surface to allow a SiO_2 layer to form, resulting in electrochemical polishing. Although a number of variations on this etching mechanism have been proposed [2], the critical step in determining whether PSi formation or electrochemical polishing occurs remains a competition between kinetics of the chemical dissolution of fluorinate terminal silicon atoms versus the rate of SiO_2 formation, with the transition between the two processes being generally believed to occur at the J_{ps} peak in the I–V curve. In all the mechanisms the dissolution valence value for PSi is predicted to be two, whilst for electrochemical polishing it should be four [2]. However, actual measurements of the dissolution valence reveal values greater than two prior to the appearance of the J_{ps} peak, at current densities around 50% of J_{ps}, indicating a mixture of PSi formation and electropolishing. Furthermore, it has been reported that the flat-band potential (likely negative limit for the possible onset of oxide growth) occurs negative to the U_{ps} potential and Zhang found that complete coverage by PSi only occurs in the early exponential region [22–24]. These observations suggest that some silicon oxide can already form prior to the obtaining of the U_{ps} potential and this is further supported by the appearance of Si–O bands in the FTIR spectra (Fig. 5). It is thus postulated here that some oxide starts to form shortly after the switch from exponential to linear behaviour in the I–V curve, i.e. the potential region where the dramatic changes in the PL spectra and average nanocrystal size occur.

However, Lewerenz et al., on the basis of FTIR and photoelectron spectroscopy data, specifically ruled out the possibility of SiO_2 formation prior to U_{ps} [25,26]. Although these workers were using different conditions, n-type silicon in 0.1 M NaF (pH 4.0) or diluted NH_4F, it is not easy to explain the contradiction between the two sets of data. Despite the precautions taken to avoid atmospheric oxidation during the present experiments, the possibility of its occurrence cannot be completely excluded, especially as the oxide films observed were very thin; Ozanam and Chazalviel reported that a perpendicular Si–O stretching mode at 1170 cm^{-1} would indicate sub-monolayer coverage [27]. Nevertheless, the fact that partial oxide films were only found on PSi specimens formed at 80 mV and not on those grown at 0 mV suggests that oxidation occurs during the etching process rather than from subsequent contamination by atmospheric oxygen. Finally, note that Lewerenz et al. did detect some Si–OH bonds as the bias potential approached U_{ps}, indicating that these are no longer immediately converted to Si–F bonds [25]. A longer lifetime for the Si–OH bonds is a precursor for oxide formation [21].

It is generally accepted that the size of the nanocrystals in a microporous silicon film is controlled by quantum confinement effects. In the absence of illumination, the minimum size should be inversely proportional to the applied field [2]. Quantum confinement models thus predict a gradual decrease in the average crystallite size, causing a continuous blue-shift in the PL spectra, with increasing applied potential and thus it cannot explain the sudden changes observed in this work. However, the majority of the quantum confinement models presented to date assumed that charge transfer involves silicon atoms terminated by hydrogen (S–H), rather than oxygen terminated (Si–OH or Si–O), i.e. the condition proposed above to exist at potentials approaching U_{ps}.
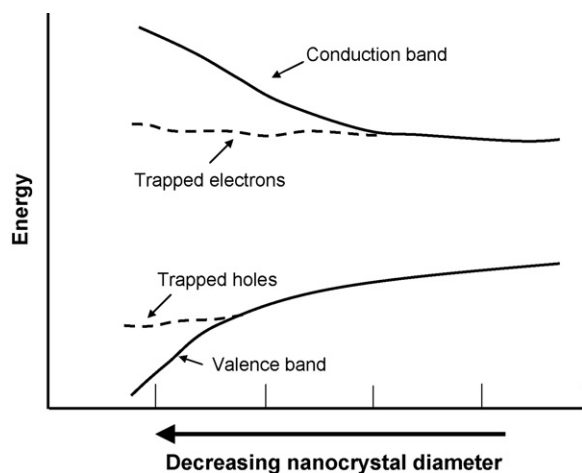
Fig. 6. Schematic representation of the Wolkin's model for oxygen terminated PSi in which trapped exciton states dominate the PL behaviour of the smallest nanocrystals [14].

Conversely, Wolkin et al. [14,15] investigated the influence of oxygen on the PL properties and electronic structure of PSi and claimed that for PSi terminated by Si=O bonds a critical size exists (in the range 1.5–3.0 nm) below which PL recombination processes involve trapped mid bandgap states, rather than the valance and conduction bands (Fig. 6). Since the energy of the trapped exciton states are independent of crystallite size, for very small oxygen terminated PSi there is no longer a relationship between PL energy and particle size.

It is now proposed here that these trapped exciton states of oxygen terminated PSi can participate in the electrochemical etching process, which should be possible if the trapped holes states are below the Fermi level. Therefore once a sufficiently large field is applied to form oxygen terminated nanocrystal smaller than the critical size for the trapped exciton states to move into the bandgap, these can continue to shrink without any additional increment in the magnitude of the applied field, i.e. their minimum size will no longer be restricted by quantum confinement. Hence a sudden drop in the average nanocrystallite size can be anticipated to occur at some critical potential somewhere between the flat-band potential and U_{ps}, which is consistent with the TEM data (Table 2).

Of course the removal of the quantum confinement restrictions on the minimum particle size could lead to electropolishing, but this still has to compete with the chemical conversion of the Si–OH to Si–F, i.e. the literature mechanism for PSi formation, which would re-establish a Si–H terminated surface and thus re-instate the quantum confinement size restrictions and thereby prevent the complete dissolution of the nanocrystals. Therefore electropolishing would only be expected at high current densities, i.e. >J_{ps}. Thus the involvement of mid bandgap states in the etching process can explain:

- the step function observed in the plot of average nanocrystallite size against applied potential;
- and the corresponding dramatic blue-shift in the PL spectrum (Fig. 2).

5. Conclusions

It has been found that when PSi is potentiostatically formed by electrochemical etching in dilute HF, a dramatic decrease in the average nanocrystal size, as evidenced by both a blue-shift in the peak PL wavelength and direct measurements via HRTEM, occurs in a short potential range. Furthermore, this takes place after the current density switches from an exponential dependence on the applied potential to a linear relationship, but importantly prior to reaching the U_{ps} potential (usually consider the onset of electropolishing). This rapid decrease in particle sizes was explained in terms of the partial formation of an oxide film and invoking the trapped exciton states model for oxygen terminated PSi proposed by Wolkin et al. [14,15], such that the minimum particle size is no longer restricted by quantum confinement. Support for the presence of a partial oxide prior to the U_{ps} comes from both previous literature related to the location of the flat-band potential and FTIR measurements carried out in the present work.

Acknowledgement

References

[1] L.T. Canham, Appl. Phys. Lett. 57 (1990) 1046.
[2] V. Lehmann, Electrochemistry of Silicon: Instrumentation, Science, Materials and Applications, Wiler-VCH Verlag GmbH, Weinheim, 2002, pp. 51–120.
[3] R.L. Smith, S.D. Collins, J. Appl. Phys. 71 (1992) R1.
[4] H. Föll, Appl. Phys. A 53 (1991) 8.
[5] V. Lehmann, Adv. Mater. 4 (1992) 762.
[6] X.G. Zhang, S.D. Collins, R.L. Smith, J. Electrochem. Soc. 136 (1989) 1561.
[7] H. Koyama, J. Appl. Electrochem. 36 (2006) 999.
[8] Z. Gaburro, H. You, D. Babic, J. Appl. Phys. 84 (1998) 6345.
[9] M. Ohmukai, Y. Tsutsumi, Jpn. J. Appl. Phys. 36 (1997) L292.
[10] N. Koshida, H. Koyama, Jpn. J. Appl. Phys. 30 (1991) L1221.
[11] T. Ban, T. Koizumi, S. Haba, N. Koshida, Y. Suda, Jpn. J. Appl. Phys. 33 (1994) 5603.
[12] D.W. Cooke, R.E. Muechausen, B.L. Bennett, L.G. Jacobsohn, M. Nastasi, J. Appl. Phys. 96 (2004) 197.
[13] G. Allan, C. Delerue, M. Lannoo, Phys. Rev. Lett. 76 (1996) 2961.
[14] M.V. Wolkin, J. Jorne, P.M. Fauchet, Phys. Rev. Lett. 82 (1999) 197.
[15] J.V. Behren, M. Wolkin-Vakrat, J. Jorné, P.M. Fauchet, J. Porous Mater. 7 (2000) 81.
[16] S. Adachi, M. Oi, J. Appl. Phys. 102 (2007) 063506.
[17] D.J. Blackwood, Y. Zhang, Electrochim. Acta 48 (2003) 623.
[18] A.G. Cullis, L.T. Canham, Nature 353 (1991) 335.
[19] Y.K. Xu, S. Adachi, J. Phys. D: Appl. Phys. 39 (2006) 4572.
[20] Y.K. Xu, S. Adachi, J. Appl. Phys. 101 (2007) 103509.
[21] P. Allongue, V. Kieling, H. Gerischer, Electrochim. Acta 40 (1995) 1353.
[22] S. Ottow, G.S. Popkirov, H. Föll, J. Electroanal. Chem. 455 (1998) 29.
[23] T.L.S.L. Wijesinghe, S.Q. Li, D.J. Blackwood, J. Phys. Chem. C 112 (2008) 303.
[24] X.G. Zhang, J. Electrochem. Soc. 151 (2004) C69.
[25] J. Rappich, H.J. Lewerenz, Thin Solid Films 276 (1996) 25.
[26] H.J. Lewerenz, M. Aggour, C. Murrell, M. Kanis, J. Jungblut, J. Jakubowicz, P.A. Cox, S.A. Campbell, P. Hoffmann, D. Schmeisser, J. Electrochem. Soc. 150 (2003) E185.
[27] F. Ozanam, J.N. Chazalviel, J. Electroanal. Chem. 269 (1989) 251.